



Reinvestigation of the thermal properties of single-crystalline SnSe

Dorra Ibrahim, Jean-Baptiste Vaney, Selma Sassi, Christophe Candolfi,
Viktoriia Ohorodniichuk, Petr Levinsky, Christopher Semprimoschnig, Anne
Dauscher, Bertrand Lenoir

► To cite this version:

Dorra Ibrahim, Jean-Baptiste Vaney, Selma Sassi, Christophe Candolfi, Viktoriia Ohorodniichuk, et al.. Reinvestigation of the thermal properties of single-crystalline SnSe. Applied Physics Letters, 2017, 110 (3), pp.032103. 10.1063/1.4974348 . hal-03969693

HAL Id: hal-03969693

<https://hal.univ-lorraine.fr/hal-03969693>

Submitted on 2 Feb 2023

HAL is a multi-disciplinary open access archive for the deposit and dissemination of scientific research documents, whether they are published or not. The documents may come from teaching and research institutions in France or abroad, or from public or private research centers.

L'archive ouverte pluridisciplinaire **HAL**, est destinée au dépôt et à la diffusion de documents scientifiques de niveau recherche, publiés ou non, émanant des établissements d'enseignement et de recherche français ou étrangers, des laboratoires publics ou privés.

Reinvestigation of the thermal properties of single-crystalline SnSe

Cite as: Appl. Phys. Lett. **110**, 032103 (2017); <https://doi.org/10.1063/1.4974348>

Submitted: 01 August 2016 • Accepted: 06 January 2017 • Published Online: 19 January 2017

D. Ibrahim, J.-B. Vaney, S. Sassi, et al.



View Online



Export Citation



CrossMark

ARTICLES YOU MAY BE INTERESTED IN

[Assessment of the thermoelectric performance of polycrystalline p-type SnSe](#)

Applied Physics Letters **104**, 212105 (2014); <https://doi.org/10.1063/1.4880817>

[Low thermal conductivity and triaxial phononic anisotropy of SnSe](#)

Applied Physics Letters **105**, 101907 (2014); <https://doi.org/10.1063/1.4895770>

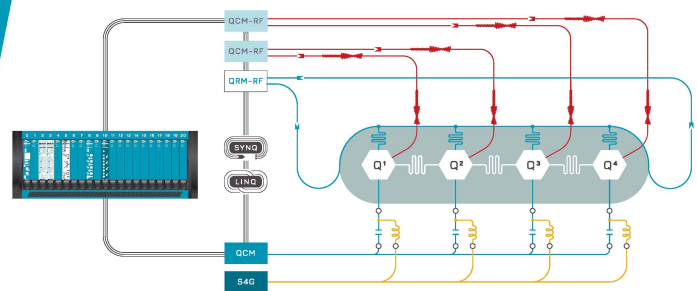
[Low temperature thermoelectric properties of p-type doped single-crystalline SnSe](#)

Applied Physics Letters **112**, 142102 (2018); <https://doi.org/10.1063/1.5023125>



Integrates all
Instrumentation + Software
for Control and Readout of
Superconducting Qubits

[visit our website >](#)



Reinvestigation of the thermal properties of single-crystalline SnSe

D. Ibrahim,¹ J.-B. Vaney,¹ S. Sassi,¹ C. Candolfi,¹ V. Ohorodniichuk,¹ P. Levinsky,¹
 C. Semprimoschnig,² A. Dauscher,¹ and B. Lenoir^{1,a)}

¹Institut Jean Lamour, UMR 7198 CNRS – Université de Lorraine, Parc de Saurupt, CS 50840, 54011 Nancy, France

²European Space Agency, ESTEC, P.O. Box 299, Keplerlaan 1, 2200 AG Noordwijk, The Netherlands

(Received 1 August 2016; accepted 6 January 2017; published online 19 January 2017)

The simple binary SnSe has been recently proposed as a prospective candidate for thermoelectric applications due to its exceptionally low lattice thermal conductivity. However, the thermal transport in single crystals was found to be significantly lower than in polycrystalline samples despite the presence of grain boundary scattering in the latter. In order to better understand the origin of this issue, we report here on a detailed characterization of the thermoelectric properties of a vertical-Bridgman-grown single-crystal of SnSe along the a , b , and c crystallographic axes in a wide range of temperatures (5–700 K). We find that the thermal conductivity features a pronounced Umklapp peak near 12 K whose magnitude depends on the crystal orientation. Unlike prior reports, our results evidence a significant anisotropy between the a , b , and c directions with lattice thermal conductivity values reaching 1.2, 2.3, and 1.7 W m⁻¹ K⁻¹ at 300 K, respectively. While the fundamental reasons behind these differences remain unclear, our results indicate that the intrinsic lattice thermal conductivity of single-crystalline SnSe is likely significantly higher than previously thought. Published by AIP Publishing. [<http://dx.doi.org/10.1063/1.4974348>]

Single crystalline SnSe has stirred up considerable interest over the last two years due to its announced record-breaking thermoelectric performances.^{1–18} This simple binary compound, crystallizing within an orthorhombic unit cell, was found to behave as a nearly intrinsic semiconductor synonymous with high electrical resistivity (ρ), high thermopower (α), and negligible electronic thermal conductivity (κ_e) in both polycrystals and single crystals.^{1,5,6} However, what makes this compound standing out among the binaries SnX ($X = S, Se, Te$), recently revisited for their interesting thermoelectric properties,^{19–22} is the extremely low lattice thermal conductivity values (κ_L) reaching 0.25, 0.3, and 0.35 W m⁻¹ K⁻¹ at 800 K along the a , b , and c crystallographic axes, respectively.¹ A recent inelastic neutron scattering investigation has shown that this low ability to conduct heat originates from a strong anharmonicity associated with the proximity of a ferroelectric-like lattice instability driven by orbital interactions.⁴ Thanks to this remarkable property, values of the dimensionless thermoelectric figure of merit ZT ($ZT = \alpha^2 T / \rho(\kappa_L + \kappa_e)$) as high as 2.6 and 2.3 were achieved at 950 K in the b and c directions, respectively.¹

Detailed investigations of the thermoelectric performances of polycrystalline samples revealed only moderate ZT values of 0.5 at 823 K.^{5,6} Further progress has been recently made with the insertion of different dopants such as Ag or Na, resulting in peak ZT values of 0.8 at 800 K in p -type 1% Na- and K-doped SnSe and 1.0 at 773 K in n -type SnSe_{0.87}S_{0.1}I_{0.03}.^{6,15,16} The main difference between the studies conducted on single crystals and polycrystals is tied to the significantly higher lattice thermal conductivity measured in the latter.^{5,6} This surprising observation is at odds with the simple expectation that grain boundary scattering should act

as an additional source of phonon scattering, resulting in lower κ_L values in polycrystals. The possible air-sensitivity of SnSe has been advanced to reconcile these contradicting results.² Another unresolved issue is the fact that no anisotropy was observed in measurements performed along the b and c axes (Ref. 1), while *ab-initio* calculations of $\kappa_L(T)$ predicted tri-axial anisotropy with the sequence $\kappa_L^a < \kappa_L^c < \kappa_L^b$.²³ Of note, the computed values along the b and c directions also differed significantly from the experimental results.²³

Motivated to determine the possible origins of these contradicting reports, we grew high-quality single crystals of SnSe by a Bridgman technique with the aim to reinvestigate the thermal properties of this compound. Herein, we report on the structural and chemical characterizations and thermoelectric property measurements along the three crystallographic directions a , b , and c in a wide range of temperatures (5–700 K). At variance with prior results, our measurements evidence that the lattice thermal conductivity values along the a , b , and c directions are significantly higher, reaching 1.2, 2.3, and 1.7 W m⁻¹ K⁻¹ at 300 K, respectively. In addition, we find a marked anisotropy between the b and c directions in agreement with *ab-initio* phonon calculations. We further discuss possible reasons for the differences observed between our results and those previously obtained.

High-quality single crystals of SnSe were grown by a vertical Bridgman method from a polycrystalline ingot of SnSe prepared from the reaction of stoichiometric amounts of Sn shots (99.999%) and Se shots (99.999%). The polycrystalline ingot (10 cm long and 10 mm diameter) was prepared following the route used in our prior study.⁴ This ingot was then inserted into a quartz tube (10 mm diameter) tapered at the bottom to favor seed selection and growth. This sealed tube was then placed inside a second quartz tube of larger dimensions. This precaution is necessary due to the structural transition undergone by SnSe at high temperatures

^{a)} Author to whom correspondence should be addressed. Electronic mail: bertrand.lenoir@univ-lorraine.fr

that breaks the inner tube upon cooling when single crystals or large grains form. The quartz tube was placed in a vertical furnace in which a temperature gradient of 20 K cm^{-1} was applied. The temperature of the hotter zone of the furnace was higher than the melting point temperature of SnSe and was kept constant during the growth process. The tube was vertically lowered through the hot zone at a speed of 4 cm per day. After completion of the process, the tube was furnace-cooled down to room temperature. No further annealing step was subsequently applied. The as-grown crystal was single-crystalline few millimeters above the tip with the a axis nearly perpendicular to the growth direction.

The crystal structure of the solidified material was confirmed by single-crystal and powder X-ray diffraction (PXRD) using a Bruker D8 Advance. The chemical homogeneity was

assessed by scanning electron microscopy (SEM) and energy-dispersive X-ray spectroscopy (EDXS) using a FEI 650 Quanta FEG. Both analyses confirmed the growth of orthorhombic SnSe and demonstrated the excellent chemical homogeneity of the crystals (Figure 1). A piece of the crystal cleaved within the bc plane (about 2 cm long and 6 mm thick) was placed on a 3-axis goniometric head and orientated by Laue diffraction. Samples for transport property measurements were cut from this piece with a diamond-wire saw along the a , b , and c crystallographic axes. Bar-shaped samples with dimensions $(5.5\text{--}6.5) \times (2.2\text{--}2.8) \times (1.2\text{--}2.2)\text{ mm}^3$ were cut for low-temperature transport measurements, which were performed between 300 and 5 K with the thermal transport option of a physical property measurement system (PPMS, Quantum Design). The electrical and thermal contacts

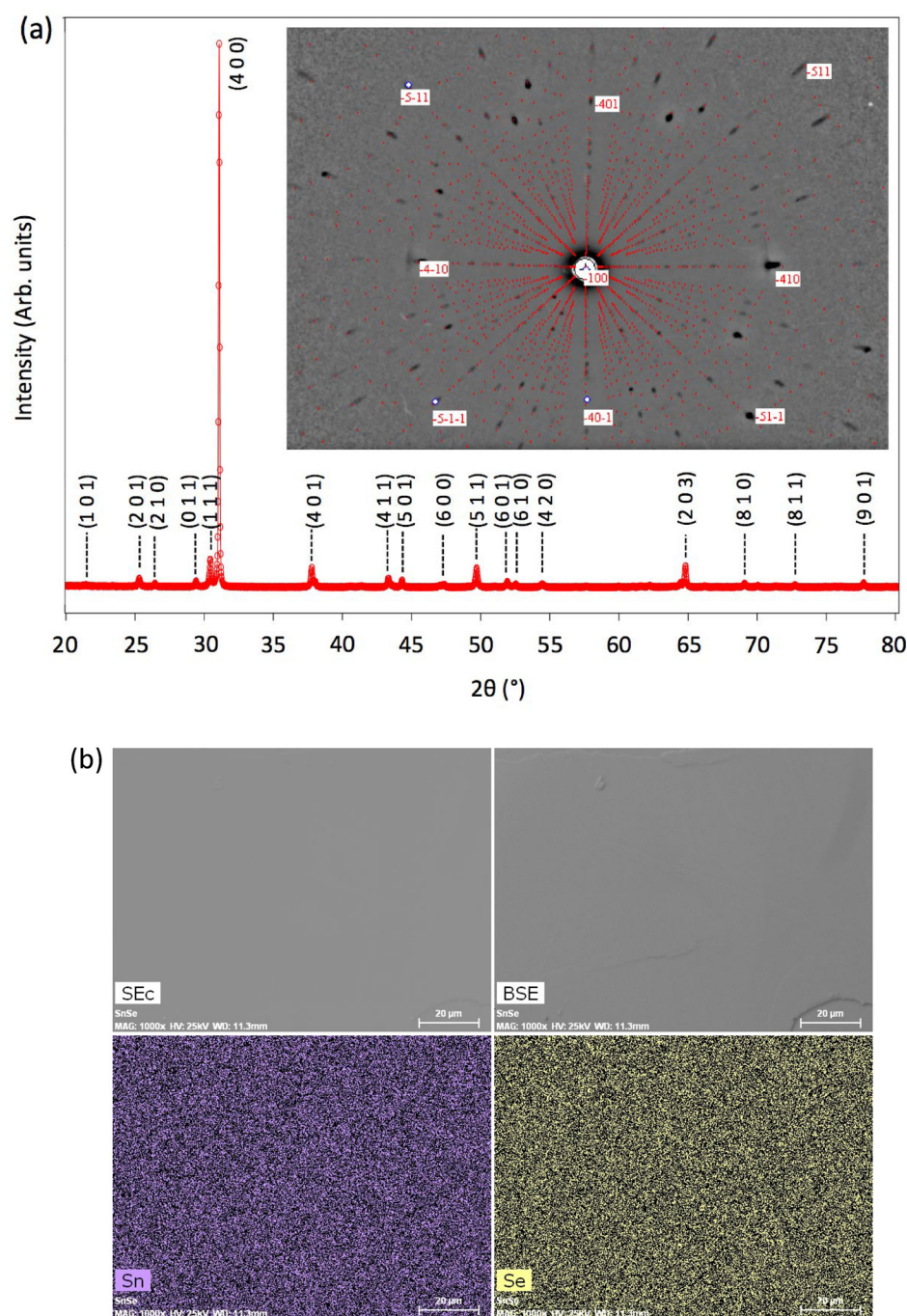


FIG. 1. (a) PXRD pattern of powdered SnSe single crystals grown via the Bridgman method. The main peaks are indexed. Inset: An example of the Laue diffraction image with the calculated pattern (in red) superimposed. (b) SEM secondary electron and backscattered electron images collected on single-crystalline SnSe together with the corresponding elemental X-ray maps, indicating the good chemical homogeneity of the crystal. For all panels, the scale bar corresponds to 20 μm .

were realized on freshly cut surfaces by gluing copper bars with silver epoxy. The same samples were used to measure the electrical resistivity and thermopower between 300 and 700 K using a ZEM-3 system (Ulvac-Riko). Square-shaped samples ($6 \times 6 \times (0.8\text{--}2)$ mm³) were cut to probe the thermal diffusivity d in the temperature range of 300–700 K using a laser flash technique (LFA 427, Netzsch). The thermal conductivity was determined by combining the thermal diffusivity, the specific heat C_P , and the density β according to the relation $\kappa = dC_P\beta$. The density, determined from weight and dimensions of the samples, was found to be 6.10 ± 0.05 g cm⁻³. As a first approximation, we have neglected the variations of β with temperature. This value is consistent with that expected from crystallographic data (ranging between 6.13 and 6.18 g cm⁻³ from X-ray and neutron diffraction data, Refs. 24 and 25), indicating that all the samples measured were fully dense. The specific heat was obtained by linearly extrapolating the data measured on a polycrystalline sample between 300 and 700 K (see below).⁵ Since both Sn-rich and Se-rich SnSe crystals can be obtained by varying the growth and annealing conditions,²⁶ the samples were cut in the same region of the grown crystal in order to limit possible variations in the carrier concentration along the long axis during the solidification process. For this reason and due to the reduced dimensions of the initial cleaved piece, the thermal transport could be only probed along the b and c directions at high temperatures.

Figures 2(a) and 2(b) show the temperature dependence of the electrical resistivity and thermopower, respectively, measured along the three crystallographic axes. The results are consistent with the semiconducting nature of undoped SnSe underlined in several studies on either polycrystals or single crystals.^{1,5,6} The slight but visible hump on the $\rho(T)$ curves above 400 K has been also observed in pristine polycrystalline and single crystalline samples.^{1,5,6} However, contrary to the results obtained by Zhao *et al.*,^{1,2} the electrical transport appears anisotropic along the b and c directions with ρ values two orders of magnitude higher that hint at a lower hole concentration in the present crystal. Early studies on SnSe single crystals have shown that the hole concentration strongly depends on the growth conditions.²⁶ Deviations from the ideal stoichiometry yield either Sn-rich or Se-rich samples with hole concentrations varying from 3×10^{15} up to 2×10^{18} cm⁻³ at 77 K.²⁶ The larger electrical resistivities

measured herein suggest a low hole concentration, *i.e.*, small deviations from the ideal stoichiometry. In agreement with the high ρ values, α reaches $850 \mu\text{V K}^{-1}$ in the b and c directions and $930 \mu\text{V K}^{-1}$ in the a direction at room temperature. The slight anisotropy seen in $\alpha(T)$ is consistent with first-principles calculations performed by Kutorasinski *et al.*¹⁸ Around 300 K, $\alpha(T)$ is maximum and starts decreasing at higher temperatures due to the thermal activation of minority carriers.

Figure 3 shows the temperature dependence of the total thermal conductivity κ measured along the three directions. In the present case, the electronic thermal conductivity κ_e estimated by the Wiedemann-Franz law ($\kappa_e = LT/\rho$ where L is the Lorenz number) is negligible in the whole temperature range since it amounts to at most 0.2% of the κ values at 800 K when considering a maximum L value of 2.45×10^{-8} V² K⁻² valid in the degenerate limit. Due to the intrinsic semiconducting nature of the present sample, the actual Lorenz number is likely significantly lower than this value, leading to an electronic contribution even lower than 0.2% at 800 K. Thus, we can safely conclude that the measured κ values solely reflect the phonon contribution. Irrespective of the crystal orientation, the $\kappa(T) \equiv \kappa_L(T)$ data feature a pronounced Umklapp peak near 12 K with a maximum value of $52 \text{ W m}^{-1} \text{ K}^{-1}$ reached along the b axis, a characteristic that has also been observed in polycrystals.²⁷ Because the amplitude of this peak is sensitive to crystal imperfections, the large values reached can be considered as an indicator of the good crystalline quality of our sample. Along the a and c directions, the peak value decreases, a lower ability to conduct heat being synonymous with a lower peak value. Measurements performed above 300 K confirm the values obtained with the PPMS, thermal radiations inherent to the low-temperature measurements being responsible for the slight discrepancy observed near 300 K between the two sets of data. Upon increasing temperature up to 700 K, $\kappa_L(T)$ monotonically decreases down to $\sim 1 \text{ W m}^{-1} \text{ K}^{-1}$ in the b and c directions.

While our results are consistent with early studies performed on single-crystalline SnSe ($1.9 \text{ W m}^{-1} \text{ K}^{-1}$ at 300 K perpendicular to the c axis),²⁸ the present results differ significantly from those reported recently (Ref. 1) in three important aspects. First, κ_L exhibits a significant anisotropy between the three directions, in particular, between the b and

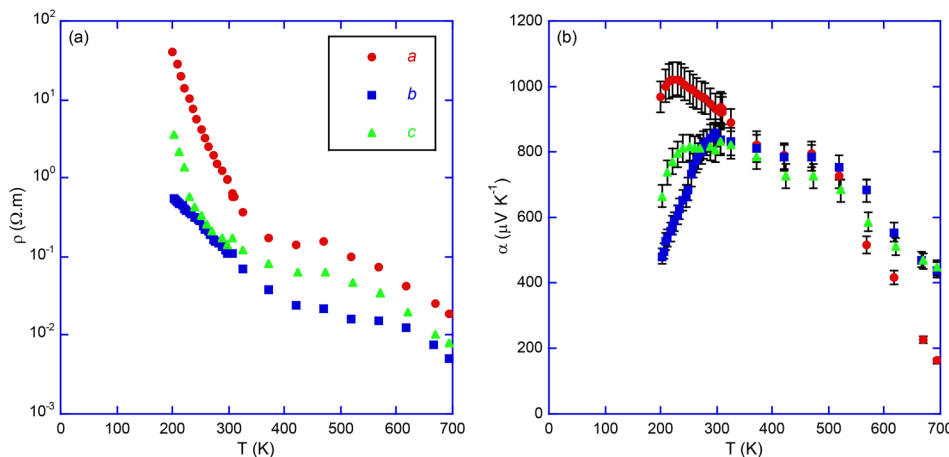


FIG. 2. Temperature dependence of the (a) electrical resistivity ρ and (b) thermopower α of single-crystalline SnSe measured along the a (circle symbol), b (square symbol), and c (triangle symbol) axes. Due to the high ρ values, both temperature dependences could be followed only down to ~ 200 K. In panel (a), the error bars are smaller than the size of the symbols used. The experimental uncertainty is estimated to be 5% for measurements at low and high temperatures.

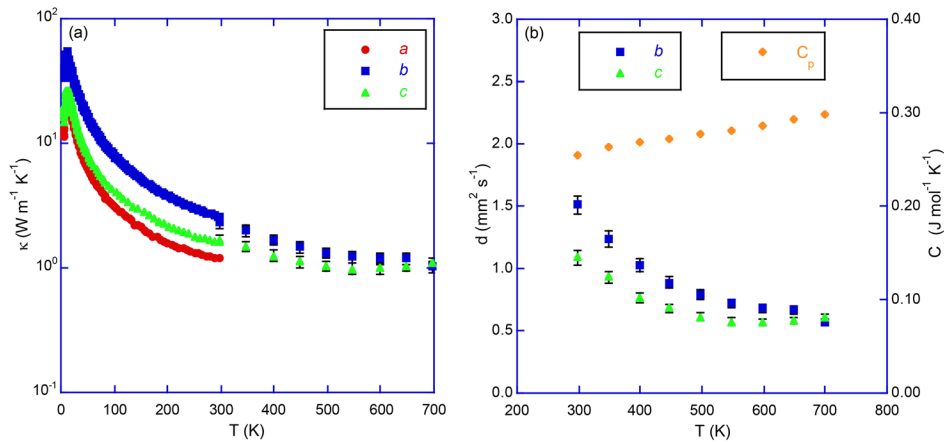


FIG. 3. (a) Temperature dependence of the total thermal conductivity κ of single-crystalline SnSe measured along the a (circle symbol), b (square symbol), and c (triangle symbol) axes. At low temperatures, the error bars are smaller than the size of the symbols used. The experimental uncertainty is estimated to be 5% and 10% for measurements at low and high temperatures, respectively. (b) Temperature dependence of the thermal diffusivity along the b and c axes and of the specific heat measured in our prior study (Ref. 5) and used in the calculation of κ .

c axes. The values follow the sequence $\kappa_L^a < \kappa_L^c < \kappa_L^b$ in perfect agreement with the predictions made by *ab-initio* calculations (in Ref. 1, the κ_L values measured along the b and c axes are nearly identical when considering the experimental uncertainty).²³ Second, the values measured at 300 K in the a , b and c directions (1.2 , $2.3 \text{ W m}^{-1} \text{K}^{-1}$ and $1.7 \text{ W m}^{-1} \text{K}^{-1}$, respectively) are between two and three times higher than those measured by Zhao *et al.*^{1,2} Third, our results are consistent with the values measured on polycrystalline samples perpendicular and parallel to the pressing directions.^{5,6,27}

We now turn to the thorny question of the possible reasons behind such large differences between the κ_L values reported herein and those obtained in prior investigations. A first mechanism evoked is related to air exposure, resulting in surface oxidation that might obscure the intrinsic signal during measurements.² Yet, we did not observe any indication of significant air sensitivity of SnSe under ambient conditions by neither X-ray diffraction nor chemical analyses. Further, the samples used for transport characterization were freshly cut before measurements with additional surface polishing shortly before gluing the contacts onto the samples or introducing the sample in the laser flash system. Finally, we note that the two different methodologies and instruments used to measure the thermal properties at low and high temperatures yield consistent results. Hence, the possible surface oxidation of the samples under ambient conditions is not thought to play a major detrimental role in thermal transport measurements.

May intrinsic defects be then at the origin of these differences? On one hand, the higher electrical resistivity and thermopower values indeed point to a lower amount of native defects in our single crystal. A large concentration of vacancies and/or antisite defects may be considered as a source of additional phonon scattering, whereby lowering the κ_L values. Recently, in a response to a comment of Wei *et al.*,²⁹ Zhao *et al.*²⁹ argued that a large amount of vacancies was present in their single crystals. Yet, the concentration of vacancies evoked (corresponding to a chemical composition of $\text{Sn}_{0.835}\text{Se}$) seems very large and still needs to be clearly confirmed experimentally. On the other hand, similar defect chemistry is known to play a prominent role in determining the electronic properties in undoped SnS, SnTe, or in Bi_2Te_3 -based alloys without strongly influencing the lattice thermal conductivity.^{19,21,22,30,31} Nevertheless, given the fact that antisite defects can play an

important role in determining the lattice thermal conductivity even at high temperatures,³² it would be very interesting to further explore this possibility by comparing the microstructure at the nanoscale by transmission electron microscopy and by probing the transport on samples cut in different areas of the single crystal in order to determine whether variations of the defect concentration and/or microstructure along the long axis of the crystal can cause such large variations in the thermal transport.

While the possibility of a strong influence of defects still exists, another intriguing point warrants further attention. Upon closer inspection of the data measured on single-crystalline undoped SnSe by Zhao *et al.*,¹ the thermal conductivity, thermal diffusivity, and specific heat data point to a density of 5.33 , 5.34 , and 5.40 g cm^{-3} in the a , b , and c directions, respectively, which corresponds to approximately 86%–88% of the theoretical density from powder X-ray diffraction or neutron diffraction data (from 6.13 to 6.18 g cm^{-3}).^{24,25} We note that Wei *et al.*²⁹ have also highlighted this point in their comment. The lower densities of the samples measured by Zhao *et al.*¹ may partly explain the lower thermal diffusivity values measured along the three directions. Our results obtained on fully dense samples suggest that the intrinsic thermal conductivity of single crystalline SnSe is significantly higher than previously thought. Clearly, further experimental efforts are necessary to determine whether the very high ZT values reported by Zhao *et al.*¹ are intrinsic to single-crystalline SnSe. In particular, a systematic comparison of the microstructure and transport properties of single crystals grown under Sn-rich and Se-rich conditions would be of interest.

D.I. greatly thanks the financial support of the Région Lorraine and the European Space Agency (ESA) through an NPI contract.

¹L.-D. Zhao, S.-H. Lo, Y. Zhang, H. Sun, G. Tan, C. Uher, C. Wolverton, V. P. Dravid, and M. G. Kanatzidis, *Nature* **508**, 373 (2014).

²L.-D. Zhao, G. Tan, S. Hao, J. He, Y. Pei, H. Chi, H. Wang, S. Gong, H. Xu, V. P. Dravid, C. Uher, G. J. Snyder, C. Wolverton, and M. G. Kanatzidis, *Science* **351**, 141 (2016).

³K. Peng, X. Lu, H. Zhan, S. Hui, X. Tang, G. Wang, J. Dai, C. Uher, G. Wang, and X. Zhou, *Energy Environ. Sci.* **454**, 9 (2016).

⁴C. W. Li, J. Hong, A. F. May, D. Bansal, S. Chi, T. Hong, G. Ehlers, and O. Delaire, *Nat. Phys.* **11**, 1063 (2015).

⁵S. Sassi, C. Candolfi, J.-B. Vaney, V. Ohorodniichuk, P. Masschelein, A. Dauscher, and B. Lenoir, *Appl. Phys. Lett.* **104**, 212105 (2014).

- ⁶C.-L. Chen, H. Wang, Y.-Y. Chen, T. Day, and G. J. Snyder, *J. Mater. Chem. A* **2**, 11171 (2014).
- ⁷E. K. Chere, Q. Zhang, K. Dahal, F. Cao, J. Mao, and Z. Ren, *J. Mater. Chem. A* **4**, 1848 (2016).
- ⁸Y.-M. Han, J. Zhao, M. Zhou, X.-X. Jiang, H.-Q. Leng, and L.-F. Li, *J. Mater. Chem. A* **3**, 4555 (2015).
- ⁹T.-R. Wei, C.-F. Wu, X. Zhang, Q. Tan, L. Sun, Y. Pan, and J.-F. Li, *Phys. Chem. Chem. Phys.* **17**, 30102 (2015).
- ¹⁰Y. Lu, J. Xu, G.-Q. Liu, J. Ynag, X. Tan, Z. Liu, H. Qin, H. Shao, H. Jiang, B. Liang, and J. Jiang, *J. Mater. Chem. C* **4**, 1201 (2016).
- ¹¹S. R. Popuri, M. Pollet, R. Decourt, F. D. Morrison, N. S. Bennett, and J. W. G. Bos, *J. Mater. Chem. C* **4**, 1685 (2016).
- ¹²H. Leng, M. Zhou, J. Zhao, Y. Han, and L. Li, *J. Electron. Mater.* **45**, 527 (2016).
- ¹³H.-Q. Leng, M. Zhou, J. Zhao, Y.-M. Han, and L.-F. Li, *RSC Adv.* **6**, 9112 (2016).
- ¹⁴X. Wang, J. Xu, G. Liu, Y. Fu, Z. Liu, X. Tan, H. Shao, H. Jiang, T. Tan, and J. Jiang, *Appl. Phys. Lett.* **108**, 083902 (2016).
- ¹⁵T.-R. Wei, G. Tan, X. Zhang, C.-F. Wu, J.-F. Li, V. P. Dravid, G. J. Snyder, and M. G. Kanatzidis, *J. Am. Chem. Soc.* **138**, 8875 (2016).
- ¹⁶Q. Zhang, E. K. Chere, J. Sun, F. Cao, K. Dahal, S. Chen, G. Chen, and Z. Ren, *Adv. Energy Mater.* **5**, 1500360 (2015).
- ¹⁷J. H. Kim, S. Oh, Y. M. Kim, H. S. So, H. Lee, J.-S. Rhyee, S.-D. Park, and S.-J. kim, *J. Alloys Compd.* **682**, 785 (2016).
- ¹⁸K. Kutorasinski, B. Wiendlocha, S. Kaprzyk, and J. Tobola, *Phys. Rev. B* **91**, 205201 (2015).
- ¹⁹G. Tan, F. Shi, S. Hao, H. Chi, L.-D. Zhao, C. Uher, C. Wolverton, V. P. Dravid, and M. G. Kanatzidis, *J. Am. Chem. Soc.* **137**, 5100 (2015).
- ²⁰R. Al Rahal Al Orabi, N. A. Mecholsky, J. Hwang, W. Kim, J.-S. Rhyee, D. Wee, and M. Fornari, *Chem. Mater.* **28**, 376 (2016).
- ²¹Q. Tan, L.-D. Zhao, J.-F. Li, C.-F. Wu, T.-R. Wei, Z.-B. Xing, and M. G. Kanatzidis, *J. Mater. Chem. A* **2**, 17302 (2014).
- ²²S. Bhattacharya, N. S. Gunda, R. Stern, S. Jacobs, R. Chmielowski, G. Dennler, and G. K. Madsen, *Phys. Chem. Chem. Phys.* **17**, 9161 (2015).
- ²³J. Carrete, N. Mingo, and S. Curtarolo, *Appl. Phys. Lett.* **105**, 101907 (2014).
- ²⁴K. Adouby, C. Perez-Vicente, and J. C. Jumas, *Z. Kristallogr.* **213**, 343 (1998).
- ²⁵T. Chattopadhyay, J. Pannetier, and H. G. von Schnering, *J. Phys. Chem. Solids* **47**, 879 (1986).
- ²⁶H. Maier and D. R. Daniel, *J. Electron. Mater.* **6**, 693 (1977).
- ²⁷S. Sassi, C. Candolfi, J.-B. Vaney, V. Ohorodniichuk, P. Masschelein, A. Dauscher, and B. Lenoir, *Mater. Today* **2**, 690 (2015).
- ²⁸J. D. Wasscher, W. Albers, and C. Haas, *Solid State Electron.* **6**, 261 (1963).
- ²⁹P.-C. Wei, S. Battacharya, J. He, S. Neeleshwar, R. Podila, Y. Y. Chen, and A. M. Rao, *Nature* **539**, E1–E2 (2016).
- ³⁰T. Caillat, M. Carle, P. Pierrat, H. Scherrer, and S. Scherrer, *J. Phys. Chem. Solids* **53**, 1121 (1992).
- ³¹T. Caillat, M. Carle, D. Perrin, H. Scherrer, and S. Scherrer, *J. Phys. Chem. Solids* **53**, 227 (1992).
- ³²A. Katre, J. Carrete, and N. Mingo, *J. Mater. Chem. A* **4**, 15940 (2016).